Magnetic Refrigeration Development

D. D. Deardorff and D. L. Johnson
Radio Frequency and Microwave Subsystems Section

Magnetic refrigeration is being developed to determine whether it may be used as an alternative to the Joule-Thomson circuit of a closed cycle refrigerator for providing 4 K refrigeration. An engineering model 4-15 K magnetic refirgerator has been designed and is being fabricated. This article describes the overall design of the magnetic refrigerator.

I. Introduction

Much interest has been generated in the past few years to develop adiabatic demagnetization into a reliable and efficient, continuous refrigeration stage for a closed cycle refrigerator. Until recently adiabatic demagnetization, or magnetic cooling, was basically regarded as a research tool, a one-shot device to producing extremely low temperatures for short periods of time. The pioneering work by Heer et al. (Ref. 1) in 1954 resulted in the first magnetic refrigerator to provide continuous low temperature (<1 K) refrigeration needed for physics research. Much of the present developmental work on continuous magnetic refrigerators centers on low temperature devices to cool infrared bolometers to below 0.3 K for spacecraft operation (Refs. 2, 3, 4), or to provide superfluid helium refrigeration (Refs. 5, 6, 7, 8) for enhancing the operation of superconducting devices, such as magnets, energy storage rings and transmission lines. All of these devices use liquid helium (^{3}He, ^{4}He or superfluid ^{4}He) as the high temperature heat reservoir.

Only very recently has the production of 4 K refrigeration using magnetic cooling been addressed. This temperature regime is generally reserved for the passively operating, but inherently inefficient, Joule-Thomson valve. A detailed analysis on a design for a 4-15 K magnetic refrigerator stage to complement a 15 K precooler was first presented in 1966 by Van Geuns (Ref. 9); however, any developmental work which may have followed has never been reported in the open literature. J. A. Barclay of the Los Alamos National Scientific Laboratory is presently pursuing the rotational magnetic wheel concept (private communication). His gadolinium gallium garnet (GGG) wheel is slowly rotated through a high magnetic field to achieve a 4-20 K temperature span. Helium gas is pumped through GGG matrix at the two temperature extremes to provide the heat exchange mechanism. Hashimoto et al. at the Tokyo Institute of Technology have recently presented experimental results obtained from a 4.2-20 K magnetic refrigerator they developed (Ref. 10). They have elected to ramp the magnetic field in order to keep their GGG matrix stationary. A helium thermosiphon extracts heat from the load; helium gas is used to transfer heat to the 20 K heat reservoir. Chinese workers are reportedly (Ref. 11) developing a 4-15 K magnetic stage to mount to a Gifford-McMahon precooler. No additional information about their work is known.

The Jet Propulsion Laboratory (JPL) has been using 1 Watt at 4.5 K closed cycle refrigerators (CCRs) since 1965 for cooling the low-noise maser amplifiers required to receive very weak signals from spacecraft in deep space. Up to 30 CCRs are in near continuous operation in the Deep Space Communications Network (DSN), logging approximately one quarter of a million hours annually. To meet the continuing requirement to increase both the reliability and efficiency of the CCR and to reduce life-cycle costs and achieve future technical objectives, JPL has initiated the development of a 4-15 K magnetic refrigerator for use with a 15 K expansion engine. This new technology is being pursured to surpass the Joule-Thomson circuit in terms of efficiency, reliability, and achievable temperature span. The decision to develop a reciprocating device stems from the long experience JPL has with the reciprocating Gifford-McMahon expansion engine and its sliding seals, its relatively simpler fabrication requirements, and the greater ease with which the experimental tests results can be verified theoretically.

The concept of magnetic refrigeration was introduced in a recent TDA Progress Report (Ref. 12). That report presented a review of magnetic refrigerator designs which have either been conceptualized or built and tested. It is the objective of this article to describe the design of the engineering model 4-15 K magnetic refrigerator under development at JPL, the component test results and the status of the development effort.

II. Principle of Magnetic Refrigeration

The placement of a paramagnetic material in a magnetic field at low temperatures causes the material to warm up. Conversely, removal of the material from the magnetic field will cause the material to cool. If the paramagnetic material is held in contact with a constant temperature reservoir, the material will tend to expel or absorb heat from the reservoir as the changing magnetic field warms or cools the material beyond the temperature of the reservoir. This is the principle of operation for the magnetic refrigerator illustrated in Fig. 1. In this figure, the magnetic refrigerator operates ideally in a Carnot cycle. Panel 1 of the figure shows the paramagnetic material thermally isolated from the precooler (heat sink) and the load (heat reservoir). As the magnetic field is increased, the temperature of the material is increased. As the material's temperature reaches that of the precooler (T_H), contact is made between the material and the precooler so that the heat of magnetization created in the material during further magnetization is removed to the precooler (Panel 2). The paramagnetic material, now at T_H and in a strong magnetic field, is again isolated (Panel 3). A reduction in the magnetic field lowers the material's temperature until it reaches the temperature (T_C) of the load. Contact is then established with the load and, during further demagnetization, the cooling of the paramagnetic material draws heat from the load (Panel 4). Thermal contact is then broken and the cycle is started over again as in Panel 1. This cyclic operation for the paramagnetic material GGG is illustrated in the entropy-temperature diagram shown in Fig. 2.

III. Experimental Design

Choice of the magnetic refrigerator design must depend ultimately on the device it is to cool, in this case the maser, an ultrasensitive microwave signal amplifier whose performance depends critically on a stable DC magnetic field and a stable, low operating temperature. Operating in the DSN, the maser is located in the feedcone of a large antenna. The antenna may be oriented from zenith to horizon for tracking purposes. The overall cooling system requirements for the maser, listed in Table 1, are therefore quite stringent. The design of the engineering model magnetic refrigerator has addressed only the basic requirements of refrigeration capacity, DC field stability, reliability, and efficiency.

The schematic of the engineering model magnetic refrigerator design is shown in Fig. 3. The major components of the refrigerator include the piston and cylinder assembly for the paramagnetic material, the drive mechanism for the piston, the superconducting magnet, the gas pumps for the low and high temperature gas circuits, and the two stage CTI Model 1020 expansion engine. The CTI Model 1020 expansion engine provides the high temperature heat sink for the magnetic refrigerator and is capable of producing better than 9 W of refrigeration at 15 K. This refrigeration capacity is a major determining factor in the final 4 K cooling power of the magnetic refrigerator. The hydrogen heat switch is used during initial cooldowns to precool the helium dewar and magnet assembly to 20 K before liquid helium is transferred into the dewar. This design presently calls for the external transfer of helium; future designs call for the magnetic refrigerator stage to provide the parasitic refrigeration requirements of the magnet. The magnet assembly (superconducting magnet and Hiperco[1]) provide the large magnetic field needed for the paramagnetic material. The piston contains two chambers filled with porous matrices of the paramagnetic material. These matrices are alternately driven into the magnetic field in a reciprocating motion by the mechanical drive system (gearmotor and a "ball reverser"[2]). Coupling the gearmotor to the ball reverser is a rotary ferrofluidic seal[3] which functions as a vacuum feedthrough to prevent contamination of the helium gas. Gas pumps in the low and high temperature gas flow loops provide the gas flow needed for the heat exchange.

The 7 T magnetic field for the GGG piston is provided by a 10.2 cm NbTi solenoid having a 6.3 cm bore. The magnet is encased with a magnetically soft material, Hiperco, having a

[1] Hiperco is an iron-cobalt alloy available from Carpenter Steel.

[2] Ball Reverser is a trade name of a mechanical actuator patented by Norco, Inc.

[3] A vacuum rotary seal patented by Ferrofluidics Corporation.

maximum permeability of 10,000 and a saturation induction of 2.4 T (see Fig. 4). The Hiperco is used as a low reluctance path to entrap much of the magnetic flux exiting from the bore of the magnet. This provides a rapid transition between the high field and low field regions enabling a shortened stroke length for the GGG piston. Figure 5 compares the measured axial profile of the magnetic field with and without the Hiperco and shows the position of the piston at the end of the stroke. The figure shows the ability of the Hiperco to shape the field, enhancing the field fall-off rate outside the magnet while slowing the fall-off rate of the field inside the magnet, although the latter effect was not as pronounced as expected. Further field shaping can be obtained by varying the shape of the Hiperco material on the ends of the magnet.

The magnet was wound with single strand 0.254/0.406 mm NbTi wire around a copper coil former. The wire was wet-wound with GE 7031 varnish to prevent motion of the individual wires during magnet charging. After winding, the magnet was potted with Stycast 2850GT. The magnet required only a small amount of training to achieve 7 T field; however, with the addition of the Hiperco, the magnet required some retraining to again reach the 7 T field. A persistent switch for the magnet has a resistance of less than 0.2 μohms corresponding to a minimum five year decay time for the magnet. A resistive shunt made from a short length of stainless steel tubing is connected to the magnet coil leads in the 4.2 K bath. The shunt resistance is chosen to protect the coil during quench while slowly dumping the 10 kJ of stored energy into the liquid helium bath.

In the cylinder assembly of the 4–15 K magnetic refrigerator, two chambers containing porous matrices of a paramagnetic material are located in tandem on a single reciprocating piston machined from phenolic (Fig. 6). In this design, each matrix volume is 33 mm long and 38 mm in diameter and is filled to about a 40% porosity with 160 grams of 1.1 mm diameter $Gd_3Ga_5O_{12}$ (GGG) spheres. The use of the two matrices effectively doubles the heat removal capabilities per cycle of the piston and reduces the temperature fluctuations by providing for a more continuous removal of energy from the heat source. The cooling power at 4.2 K for this refrigerator operating ideally in the Carnot cycle can be given as

$$\dot{Q}_C = (T_C/T_H)\,\dot{Q}_H\,\eta = 1.76\ \mathrm{W}$$

where T_C is the refrigeration temperature, T_H is the sink temperature, $\dot{Q}_H$ is the rate of heat rejection, η is the fraction of carnot efficiency at which the magnetic refrigeration stage operates, and where the CTI 1020 limits the heat expelled at 15 K to 9 W. The efficiency (assumed to be 70%) is determined by factors such as the thermal heat leaks along the cylinder and drive shaft walls, the heat exchange between the gas and the matrices, the heat capacity of the gas entrained in the matrices, and gas leakage by the seals, as well as other factors. The factors contributing to the loss of cooling power of the refrigerator will be identified and minimized during refrigerator testing.

The GGG matrices in the piston are separated sufficiently so that at either end of the stroke one matrix is in the high field region while the other matrix is in the low field region. The placement of the GGG matrices on either side of the magnet's center provides force compensation to reduce the overall force exerted on the piston drive shaft to move the piston. The magnetic interaction force that attracts the GGG to the magnet is substantial (an estimated force of 1550 newtons [350 pounds] is required to move one of the 160 gram GGG matrices through the 7 T field produced by this superconducting magnet); thus careful consideration of the separation distance between the matrices is required to greatly reduce the net magnetic force. The basic equation for the magnetic force is

$$\mathbf{F} = (\mathbf{M} \cdot \nabla)\mathbf{B}$$

where **M** is the field and temperature dependent magnetization of the paramagnetic material, and **B** is the magnetic field. Thus as a first order guesstimate, the separation of the matrices should coincide with the separation distance between the maxima in the field gradient on either side of the magnet. Figure 7 shows an initial measurement wherein a 880 N force was required to move the piston through a 7 T field (similar to the profile shown in Fig. 5 produced by the Hiperco-encased magnet). The curve represents the magnitude of the force on the piston throughout the length of the stroke. A reduction in the magnitude of the net force to less than 450 N (100 lb) is desired to ensure smooth operation of the piston's drive mechanism. This is being pursued through force compensation methods which include changing the separation distance between the GGG matrices and by reshaping the field profile by changing the shape of the Hiperco end pieces of the magnet assembly. If required, an additional force compensation method, involving the placement of small slugs of GGG between the two matrices but thermally isolated so as not to become part of the refrigeration process, will be implemented.

The GGG piston is driven with a speed-controllable gearmotor having a maximum rotation rate of 10 rad/s. This rotational motion is converted to reciprocating motion by means of a commercially available "ball reverser," a nut with ball bearings that run in a cross-hatched track cut into the drive shaft. The track has a set stroke length of 9.2 cm and the angle of the track is set to provide a displacement 3.175 cm/2π rad. This permits a maximum linear speed of 5.1 cm/s for the GGG piston. A turn-around in the ends of the track automatically reverses the direction of travel of the nut to provide smooth reciprocating motion without changing direction of rotation of the drive motor.

Heat exchange with either matrix is accomplished with helium gas provided by a separate bidirectional displacer (gas pump) in both the low and high temperature gas circuits. When the GGG piston is positioned to be adjacent to a port in the cylinder, a gas flow loop occurs. The indents in the outer surface of the piston in the area of the helium flow apertures allow the helium gas to flow through the porous matrices while the displacer is still in motion so that the gas flow need not occur only when the displacer is stalled at the ends of the stroke. The outer ridges of the piston form close tolerance seals to help prevent gas leakage along the cylinder wall. The seals further insure that gas leakage is minimized between the two gas loops. The design of the piston and gas circuitry is such that no mechanical cryogenic valves are required.

The two gas pumps (Fig. 8) are driven electromagnetically in phase relation to the motion of the GGG piston. Samarium cobalt permanent magnets are inserted in each end of the phenolic rod extending axially from the displacer. The coils are then energized with DC current in switched alternate directions to drive the displacer back and forth. The coil designs are being optimized to minimize the I^2R resistive heating in the coils. Superconducting NbTi coils are being tested for use with the low temperature gas pump. The volume displacement required of each pump was determined by

$$\dot{V} = \frac{\dot{Q}}{(\rho C_p \Delta T)}$$

where $\dot{V}$ is the volume flow rate of helium in the gas loop, ρ is the helium gas density, $\dot{Q}$ is the quantity of heat to be removed, C_p is the helium specific heat at constant pressure, and ΔT is the temperature change of the gas as it passes through the matrix. Volume displacements of 100 cc and 350 cc for the cold and warm temperature pumps were chosen assuming ΔT_C = 0.5 K and ΔT_H = 1.0 K and adding the dead volume for half of the corresponding gas loop.

The magnetic refrigerator has been designed to acheive high reliability. The magnetic refrigerator stage is a closed gas loop system; the gas circuit is sealed after the initial charge of helium gas. Internal gas displacers provide the movement of the gas through the circuitry, eliminating the need for an external compressor to provide the gas flow. The external and internal portions of the piston drive train are coupled together through a rotary seal to prevent gas contamination through the housing along the drive shaft. The magnetic refrigerator requires no small orifices as needed in the conventional Joule-Thomson valve, further minimizing the problems associated with gas contamination. Finally, the magnetic refrigerator will operate at slow reciprocating speeds, minimizing the wear rate of the low-temperature sliding seals.

IV. Conclusions

The design of a reciprocating magnetic refrigerator to pump heat from 4-15 K has been presented. The individual components have been designed and have been fabricated. Tests are underway to optimize the field profile and the placement of the GGG matrices within the piston. The assembly of the magnetic refrigerator has been initiated. With the experimental results that will be forthcoming, a careful analysis of this magnetic refrigerator concept can be used to design an efficient magnetic refrigerator usable for cooling maser amplifiers.

References

1. C. V. Heer, C. B. Barnes, and J. G. Daunt, The design and operation of a magnetic refrigerator for maintaining temperatures below 1 K, *Rev. Sci. Instrum.* 25:1088 (1954).

2. R. D. Britt and P. L. Richards, An adiabatic demagnetization refrigerator for infrared bolometers, *Int. J. Infrared Millimeter Waves* 2:1083 (1981).

3. S. Castles, Design of an adiabatic demagnetization refrigerator for studies in astrophysics, NASA/Goddard Space Flight Center Report No. X-732-80-9 (1980).

4. P. Kittel, Temperature stabilized adiabatic demagnetization for space applications, *Cryogenics* 20:599 (1980).

5. J. A. Barclay, O. Moze, and L. Paterson, A reciprocating magnetic refrigerator for 2-4 K operation: Initial results, *J. Appl. Phys.* 50:5870 (1979).

6. W. P. Pratt, Jr., S. S. Rosenblum, W. A. Steyert, and J. A. Barclay, A continuous demagnetization refrigerator operating near 2 K and a study of magnetic refrigerants, *Cryogenics* 17:689 (1977).

7. R. Beranger, G. Bon Mardion, G. Claudet, C. Delpeuch, A. F. Lacaze, and A. A. Lacaze, A gadolinium gallium garnet double acting reciprocating magnetic refrigerator, in *Advances in Cryogenic Engineering, Vol. 27*, Plenum Press, New York (1982).

8. A. F. Lacaze, R. Beranger, G. Bon Mardion, G. Claudet, and A. A. Lacaze, Double acting reciprocating magnetic refrigerator: recent improvements, Proceedings of CEC and ICMC: BA-2, Colorado Springs (1983).

9. J. R. Van Geuns, A study of a new magnetic refrigerating cycle, *Philips Res. Rep. Suppl.* 6:1 (1966).

10. H. Nakagome, N. Tanji, O. Horigami, T. Numazawa, Y. Watanabe, and T. Hashimoto, The helium magnetic refrigerator I: Development and experimental results, *Proceedings of CEC and ICMC: FC-10*, Colorado Springs (1983).

11. R. Longsworth, Cryocooler activities in China, in *Refrigeration for Cryogenic Sensors and Electronic Systems*, National Bureau of Standards Special Publication (1983).

12. D. L. Johnson, Magnetic refrigeration for maser amplifier cooling, in *The Telecommunications and Data Acquisition, Progress Report 42-67*, pp. 29-38, Jet Propulsion Laboratory, Pasadena, CA, Feb. 1982.

Table 1. CCR system requirements for maser cooling

Reliable
Efficient
Multiyear lifetime
Unattended operation
Rapid cooldowns
1-4 W cooling capacity
Compact
Magnetic field isolation of maser package
Low microphonics
mK temperature stability
Orientation independence
Continued operation during power failures

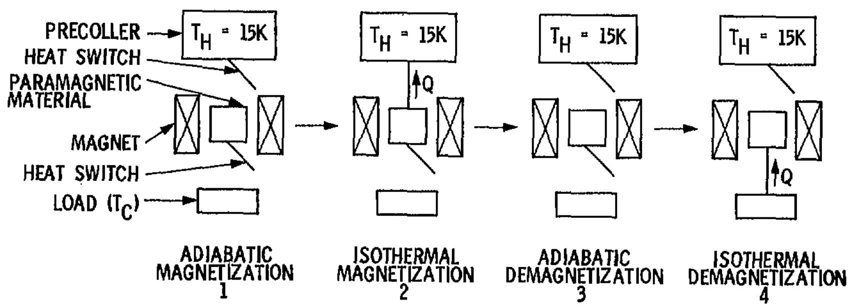

Fig. 1. Schematic of Cyclic Magnetic Refrigerator showing the refrigerator operating in the four stages of a Carnot cycle

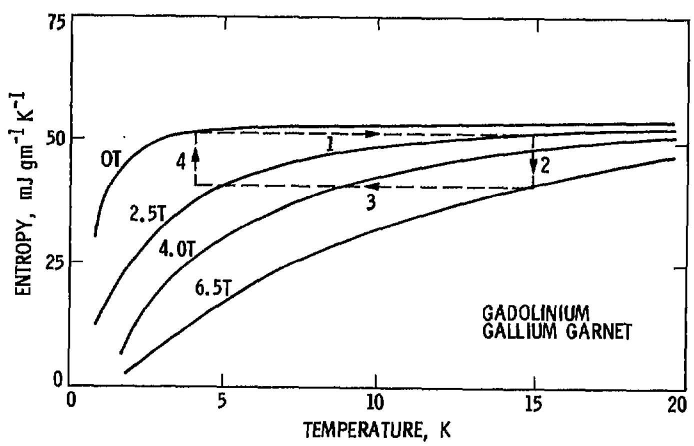

Fig. 2. S,T-diagram depicting a gadolinium gallium garnet magnet refrigerator operating in a Carnot cycle. The different stages of the Carnot cycle correspond to the illustrations of Fig. 1.

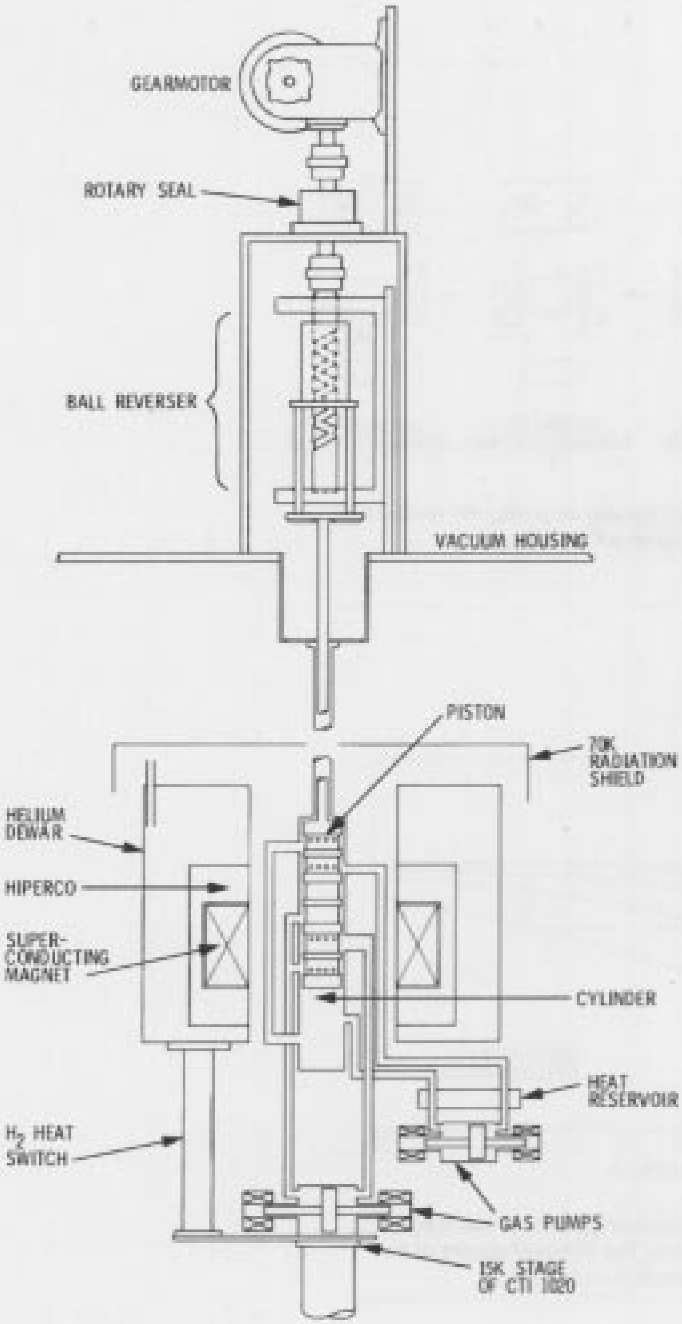

Fig. 3. Schematic of the engineering model magnetic refrigerator design

Fig. 4. Superconducting magnet/Hiperco assembly

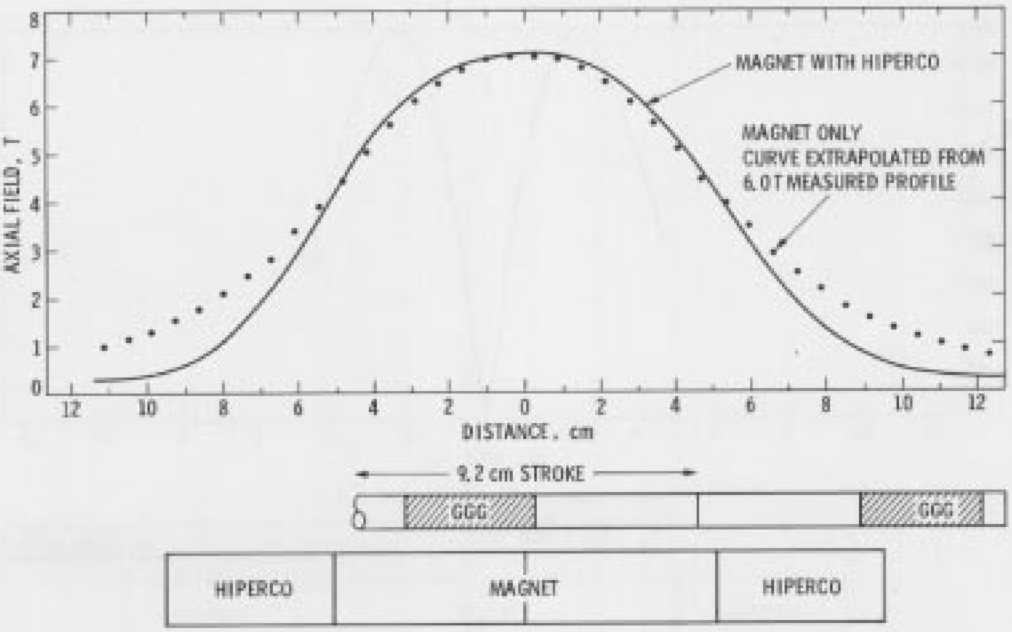

Fig. 5. Magnetic field profiles

Fig. 6. Phenolic piston containing the paramagnetic material matrices

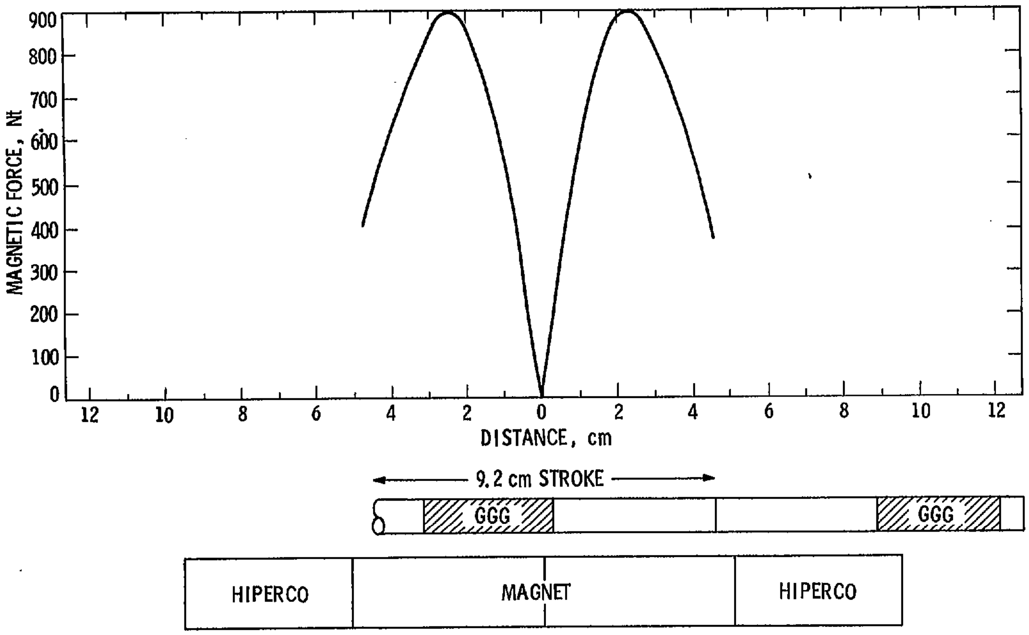

Fig. 7. Magnitude of the magnetic force acting on the piston throughout the stroke length

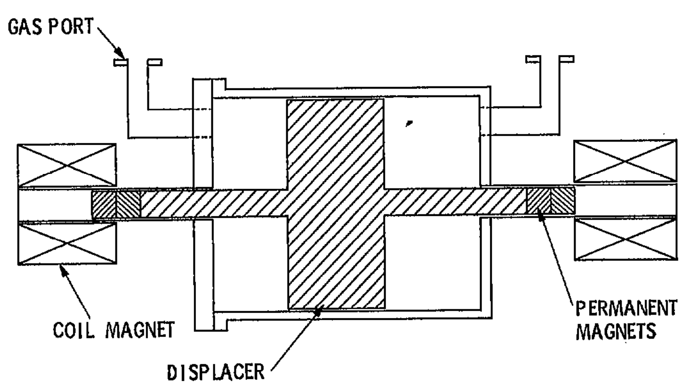

Fig. 8. Schematic of the gas pumps